

dicted is very sensitive to the value of the lab momentum, and the better the resolution of the incoming beam, the more dramatic the effect. We believe that this type of effect merits further investigation, for in addition to strengthening our faith in the present form of perturbation theory, it might turn out that many of the newly discovered "resonances," which mysteriously appear and disappear in different experiments,¹¹ are kinematical manifestations of the type discussed above.

The author wishes to acknowledge helpful discussions with Professor M. Ross, Professor M. T. Vaughn, and Dr. P. K. Srivastava.

¹P. V. Landshoff and S. B. Treiman, *Phys. Rev.* **127**, 649 (1962). We hereafter refer to this work as LT.

²In our calculations we use $M_{\omega^0} = 766$ MeV as given by E. L. Hart, R. I. Louttit, and T. W. Morris, *Phys. Rev. Letters* **9**, 133 (1962). If we use $M_{\omega^0} = 782$ MeV

as given by C. Alff *et al.*, *Phys. Rev. Letters* **9**, 322 (1962), our results must be trivially modified. The appropriate changes will be noted at the proper time.

³R. E. Cutkosky, *J. Math. Phys.* **1**, 429 (1960).

⁴B. O. Peirce and R. M. Foster, *A Short Table of Integrals* (Ginn and Company, New York, 1956), 4th ed., p. 29.

⁵If we use $M_{\omega^0} = 782$, the corresponding K^- lab momenta will be 1.21, 1.18, and 1.15 BeV/c. The qualitative features of the graphs would be the same.

⁶ $I_3(s)$ is the quantity defined by Eq. (3). $f_{\pi\lambda\Sigma}$ and $f_{KN\Sigma}$ are the pseudovector coupling constants, and $f_{\pi\omega^0\rho}$ and $f_{K\bar{K}\rho}$ are defined in reference 8. P_p and P_Σ are the particle four-momenta.

⁷J. J. Sakurai, *Ann. Phys. (N.Y.)* **11**, 1 (1960).

⁸M. Gell-Mann, *Phys. Rev.* **125**, 1067 (1962).

⁹M. Gell-Mann, D. Sharp, and W. G. Wagner, *Phys. Rev. Letters* **8**, 261 (1962).

¹⁰It is amusing to note that if the LT effect is not obscured by particle width, the amplitude for the process $K^- + p \rightarrow \Lambda + \omega^0$ may also be large because of the effect of the diagram of Fig. 1(d).

¹¹For example, see P. L. Bastien *et al.*, *Phys. Rev. Letters* **8**, 114 (1962).

SCATTERING OF MUONS FROM HYDROGEN AT LARGE MOMENTUM TRANSFER*

G. E. Masek, T. E. Ewart, J. P. Toutonghi, and R. W. Williams
Physics Department, University of Washington, Seattle, Washington
(Received 19 November 1962)

We have measured the elastic scattering cross section of 1.2-BeV/c negative muons on free protons using a beam from the Bevatron of the Lawrence Radiation Laboratory, University of California, and a pair of large liquid hydrogen targets with spark chamber detectors. The range of momentum transfers was from $5 F^{-2}$ to $18 F^{-2}$ (450 MeV/c to 850 MeV/c), and our results are therefore directly comparable with electron-proton scattering in a region in which the proton form factors have reduced the scattering cross section by about a factor of five.

Previous measurements of muon scattering^{1,2} have involved complex nuclei and lower momentum transfers; to lift these restrictions one must overcome a low-counting-rate problem [the cross section is expected to be $(2-50) \times 10^{-32}$ cm² sr⁻¹] and a possible systematic error due to pion contamination, with a cross section perhaps 10^4 times greater. A high counting rate was realized by employing two large (9 in. in diameter and 54 in. long) liquid hydrogen targets; large solid angle spark chamber detectors (typical azimuthal coverage, $\sim 20\%$); and a direct negative beam,

from an internal target, which contained a large muon flux and whose pion content was minimized by judicious adjustment of the initial beam-forming magnets. Typically, at the hydrogen targets, the beam consisted of 4000 muons and 15 000 pions per burst. The pion contamination was reduced to tolerable levels by electronic means, and the effective pion flux at the target (measured by direct observation of the scattering distribution as described below) was about 10^{-2} per burst.

The electronic rejection of pions was accomplished by a combination of accurate momentum analysis with magnets and velocity discrimination by threshold Cherenkov counters [see Fig. 1(a)]. Four gas-filled Cherenkov counters, similar to counters we have used previously,^{2,3} were part of the beam-selecting system, and a coincidence between all four was required to verify the presence of a muon. Bending magnets in the beam served both to select the required particle momentum and to sweep out knock-on electrons which otherwise would interfere with the independence of the four velocity measurements by the Cherenkov counters. A subthreshold pion

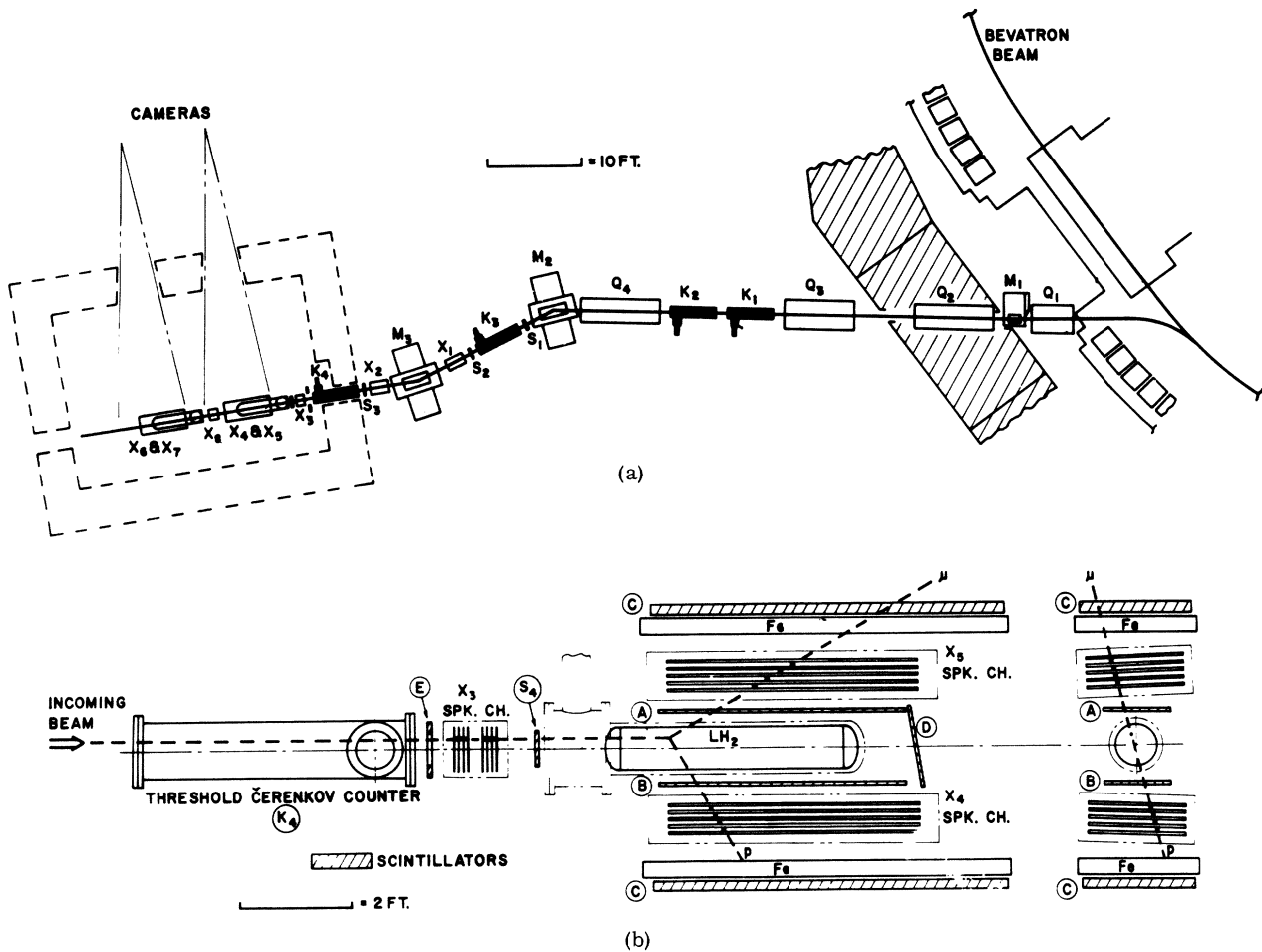


FIG. 1. (a) Layout of beam showing location of bending magnets (M), quadrupoles (Q), scintillators (S), Cherenkov counters (K), spark chambers (X), liquid hydrogen targets, and cameras. (b) Close-up of target area with scattering chambers as seen by camera. A typical elastic scattering is illustrated. The muon is shown penetrating the iron while the proton is absorbed. The end view of the track (far right) was seen by the same camera by use of mirrors, giving orthogonal views of the scattering. The spark chamber trigger was $SKABC\bar{D}E$ (see text).

can count in a Cherenkov counter if it gives rise to an energetic electron. With our standard conditions, the efficiency of a single counter for 1.2-BeV/c pions was found, both by calculation and measurement, to be about 0.02. The efficiency of a pair of counters was measured as $\sim(0.02)^2$, suggesting that the rejection of the fourfold set should be $\sim 1.6 \times 10^{-7}$. In the early stages of the experiment, direct measurements of the pion contamination in the scattering distribution indicated a much worse effective pion rejection than this. During the course of the experiment two additional sources of pion contamination were found, and were reduced to tolerable levels before the final data runs, as follows: (a) Pions of momentum appreciably higher than 1.2 BeV/c would have an enhanced efficiency in the Cheren-

kov counters and could be a serious source of contamination. Provision had already been made to measure the momentum of each beam particle directly, by placing spark chambers before and after the last bending magnet. We were thus able to restrict the useful beam to particles of accurately ($\pm 1\%$) known momentum in a well-defined range of momenta (1.05-1.40 BeV/c). (b) Despite a 30-nsec resolving time, multiple coincidences, and relatively low rates, one form of accidental coincidence was not negligible. To understand this we must first describe the triggering of the spark chambers. Figure 1(b) shows schematically the end of the beam and the liquid hydrogen target and detectors. The beam at this point has been defined by four scintillators in coincidence, $S_1 S_2 S_3 S_4 \equiv S$, four Cherenkov counters

in coincidence, $K_1K_2K_3K_4 \equiv K$, and three spark chambers X_1 , X_2 , and X_3 . An acceptable scattering event is characterized by a scattering particle (e.g., a muon) and its recoil proton counting in scintillators A and B , and the scattering particle then penetrating the 70 g cm^{-2} of iron and counting in C . The trigger is then $SKABC$. However, the large scattering cross section of pions and their large flux in the beam means that the $SABC$ rate from π 's is about 10 000 times greater than from μ 's, so the accidental in which K counts by a (nonscattered) μ and $SABC$ by a π within ± 30 nsec was appreciable. Anticoincidence counters D and E were added to prevent this effect, and the final trigger was $SKABC\overline{DE}$.

As mentioned above, an experimental check of our true pion contamination was afforded us by the nature of the π - p elastic scattering angular distribution. This allows us to state with confidence the purity of our muon sample, and to remove residual pion effects. The elastic π - p scattering⁴ near $1.2 \text{ BeV}/c$ has a pronounced rise as one goes to large angles; in the laboratory, the cross section rises from a minimum near 50° to a maximum at about 110° . In a pion scattering run (which we have performed as a check) we see nearly as many pions in the region 60° - 120° as we do in the region 22° (the minimum accepted angle) to 45° . We restrict the muon experiment to the 22° - 45° region, and we can then analyze the results in that region into a muon component and a pion component. The pion component is obtained by assuming that all scatterings over 60° are pions,⁵ and using the measured pion scattering distribution to calculate the number of pions in the 22° - 45° region.

Elastic scatterings were distinguished by the requirements of coplanarity and the relation between scattered and recoil angle for the momentum of the particle involved (the momentum in each case was known with high precision from spark chambers 1 and 2). The counters C were divided into six sections and displayed as a hodoscope on the photograph of the scattering chambers so that the penetrating particle (the muon) could be identified. Angles were measured with a precision of better than 1° , but the observed rms width of the elastic kinematic peak was 3.5° ; multiple scattering of the relatively slow recoil proton was the major contributor to this broadening. In separating elastic scatterings from the nonelastic events in the sample, we have been guided by the width of the elastic peak, and have estimated that an uncertainty of $\sim 3\%$ is introduced

into the sample in this separation.

The cross-section measurement involves the incident beam flux, distributions in momentum, angle, and space; the observed elastic scatterings at various angles; and the effective target length and solid angle product for the target and detectors at each angle. Table I summarizes the pertinent data, including the pion contamination calculation. It will be seen that the scattered-pion background was 15% of the total number of events; the error quoted for the observed yield of the scattered muon events includes the statistical uncertainty in this subtraction as well as the systematic errors such as the elastic-separation uncertainty discussed above. A number of small corrections have been included in the final result.

To compare our results with those of electron scattering, we have calculated the expected yield from the known electron-proton cross sections,⁶ the product of the calculated effective target length and the solid angle, and the measured incident beam flux. The result is the last column in Table I(b) and is shown in Fig. 2 as the ratio, R , of observed to calculated yield, at various momentum transfers.

It is clear that there is no significant evidence for a difference between muons and electrons. The total yield, for momentum transfers between $450 \text{ MeV}/c$ and $850 \text{ MeV}/c$, is 56 ± 9 , compared with an expected 48 ± 1 , and the experimental distribution has a 70% confidence level for fitting the known electron cross section. To answer the question of what sort of a difference might be expected to show up in the experiment, we must take specific models. Within the limitations of the model we can then make a comparison with muon experiments at lower momentum transfers and lower energies. In keeping with conventional analysis^{1,2} we insert a factor $(1 - 2q^2/\Lambda^2)$ in front of the Rosenbluth formula.^{7,8} We can ask either how large a Λ^{-1} would be consistent with the results, or what the most probable value (and error) on Λ^{-1} would be. Doing a χ -squared analysis on the data of Fig. 2, we find the limit (95% confidence level) allowed to a positive Λ^2 corresponds to $\Lambda = 1.2 \text{ BeV}/c$ or $\Lambda^{-1} = 0.16 \text{ F}$. If we lift the requirements that Λ^2 be positive, the best fit to the data is found for negative Λ^2 and $|\Lambda^{-1}| = (0.07 \pm 0.1) \text{ F}$. Comparable numbers from other experiments are as follows: the CERN scattering experiment¹ gives $\Lambda^{-1} = 0.28 \text{ F}$ (95%); the $g-2$ experiment,⁹ considering only the muon vertex, gives 0.17 F (95%).

The principal result of our experiment is that

Table I(a). Values of experimental parameters used in the experiment. Where parameters contribute an error to the experimental yield or a correction to the theoretical yield, these errors and corrections are listed in the last column.

Experimental parameter	Value	Correction or error ^{a,b}
Mean incident muon momenta	1.21 BeV/c	
Spread in incident momenta (including energy loss in targets)	0.07 BeV/c	+0.03
Total incident flux (sum on both targets)	3.0×10^8	
Mean angular spread in incident flux	0.6°	neg
Average vertical angle of incident flux with respect to target axis	0.5°	-0.03
Correction due to knock-on electrons counting in anti's		-0.03
Radiative correction		neg
Error in kinematic selection		± 0.03

^a + means that correction increases the "effective" muon flux in the theoretical yield calculation.

^b \pm indicates an error which has been combined with the statistical error. Neg means a negligible error.

Table I(b). Experimental and calculated yields for the experiment. The experimental yield has been corrected for pion contamination and also includes the systematic errors mentioned in Table I(a). The errors in the calculated yield arise from geometric uncertainties and are negligible for angles greater than 32° . The calculated yield also includes the corrections listed in Table I(a). The amount of pion background subtracted from the experimental yield is given in the last column.

Lab angle interval (deg)	Corrected experimental yield	Calculated yield	π background
22-26.9	21.3 ± 5.8	18.1 ± 0.9	2.7 ± 1.0
27-31.0	15.8 ± 4.9	13.4 ± 0.3	2.2 ± 0.8
32-36.9	6.2 ± 3.2	8.5	1.8 ± 0.7
37-41.9	8.8 ± 3.5	5.0	1.2 ± 0.5
42-46.9	3.4 ± 2.1	2.9	0.6 ± 0.3
greater than 47 (assumed π 's)	9.0 ± 3.0		

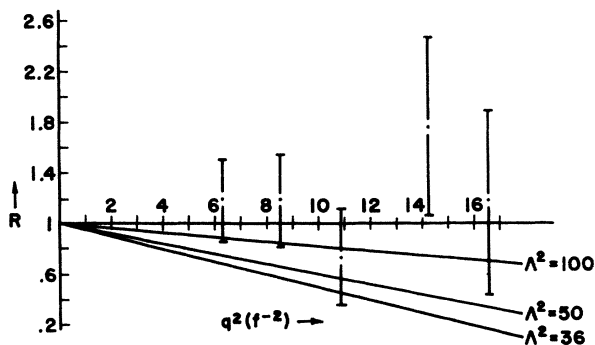


FIG. 2. R is the ratio of the observed to calculated yield and q is the momentum transfer. The lines labeled with Λ^2 values are plots of $[1 + \Lambda^2/q^2]^{-2}$ for various Λ^2 . The ratios shown include all systematic and statistical errors (see Table I).

muons scattered from free protons at momentum transfers of 450-850 MeV/c have not exhibited a behavior discernable from that of electrons.

We are indebted to our colleagues Professor H. F. Davis and Dr. E. D. Platner for many important contributions to this experiment. Assistance from R. Murano, D. Nygren, J. R. Orr, and R. O. Stenerson is gratefully acknowledged. Above all we want to thank Dr. E. J. Lofgren and the many other members of the Lawrence Radiation Laboratory staff whose fine cooperation made the experiment possible.

*Work supported in part by the National Science Foundation, the Office of Naval Research, and the U. S. Atomic Energy Commission.

¹A. Citron, C. Delorme, D. Fries, L. Goldjahl, J. Heintze, E. G. Michaelis, C. Richard, and H. Øverås, Phys. Letters 1, 175 (1962).

²G. E. Masek, L. D. Heggie, Y. B. Kim, and R. W. Williams, Phys. Rev. 122, 937 (1961).

³R. J. Swanson and G. E. Masek, Rev. Sci. Instr. 32, 212 (1961).

⁴C. D. Wood, T. J. Devlin, J. A. Helland, M. J. Longo, B. J. Moyer, and V. Perez-Mendez, Phys. Rev. Letters 6, 481 (1961).

⁵Strictly speaking we cannot prove that all particles in the high-angle region are pions. However, these particles have the correct angular distribution for pions,

and their number grows with any relaxation of the pion rejection criteria.

⁶F. Bumiller, M. Croissiaux, E. Dally, and R. Hofstadter, Phys. Rev. 124, 1623 (1961).

⁷S. D. Drell, Ann. Phys. (N.Y.) 4, 75 (1958).

⁸This could be interpreted, for example, as a muon form factor. A muon "size" or electric form factor at the muon-photon vertex would multiply the Rosenbluth formula by f_1^2 , and if we write as usual $f_1 = 1 - \frac{1}{6} \times \langle r^2 \rangle q^2 + \dots$, we see that $\langle r^2 \rangle^{1/2} = \sqrt{6} \Lambda^{-1}$.

⁹G. Charpak, F. J. M. Farley, R. L. Garwin, T. Muller, J. Sens, and A. Zichichi, Phys. Letters 1, 16 (1962).

ERRATUM

ELEMENTARY PARTICLES OF CONVENTIONAL FIELD THEORY AS REGGE POLES. Murray Gell-Mann and Marvin L. Goldberger [Phys. Rev. Letters 9, 275 (1962)].

Our expression for the contribution of a Regge pole in the u channel to the scattering of pseudo-scalar mesons by nucleons (with isotopic spin ignored) is not quite correct. In reference 9, the sign of B should be changed in Eqs. (4.17), (4.18), (4.20), and (4.21); the same is true of Eqs. (2) and (3) of our Letter.

Let us denote by P the initial nucleon four-momentum minus the final meson four-momentum and write $\not{P} = -i\gamma \cdot P$, with $P^2 = u$. The contribution to the scattering amplitude of a Regge pole of positive signature in the u channel can then be written, for large s and fixed u , as

$$\gamma_5 \frac{b(\sqrt{u})(u^{1/2} + \not{P})}{2 \sin \pi \alpha(\sqrt{u})} \left(\frac{s}{s_0}\right)^{\alpha(\sqrt{u})} \{1 + \exp[-i\pi \alpha(\sqrt{u})]\} \gamma_5$$

$$+ \gamma_5 \frac{b(-\sqrt{u})(-u^{1/2} + \not{P})}{2 \sin \pi \alpha(-\sqrt{u})} \left(\frac{s}{s_0}\right)^{\alpha(-\sqrt{u})} \{1 + \exp[-i\pi \alpha(-\sqrt{u})]\} \gamma_5,$$

in place of Eq. (2). Since $(u^{1/2} + \not{P})(2\sqrt{u})^{-1}$ and $(u^{1/2} - \not{P})(2\sqrt{u})^{-1}$ are projection operators, we may simplify and obtain

$$\gamma_5 \not{P} b(\not{P}) \left(\frac{s}{s_0}\right)^{\alpha(\not{P})} \left\{ \frac{1 + \exp[-i\pi \alpha(\not{P})]}{\sin \pi \alpha(\not{P})} \right\} \gamma_5.$$

We now introduce a neutral vector meson of mass λ coupled to the nucleon current with coupling constant $\gamma^2/4\pi$; perturbation theory to orders g^2 and $\gamma^2 g^2$ then gives, for large s and fixed u , the result

$$\gamma_5 \left\{ \frac{g^2}{\not{P} - m} + \frac{\gamma^2}{8\pi^2} g^2 \ln \left(\frac{s}{s_0}\right) \right.$$

$$\left. \times \int_0^1 \frac{dx [\not{P}(1-x) + m]}{\lambda^2(1-x) + (m^2 - \not{P}^2)x + \not{P}^2 x^2 - i\epsilon} \right\} \gamma_5.$$

[Thus, in our Eq. (4), in the formula for A , I_0 should be replaced by I_1 .] If we identify the logarithmic term as part of a series transforming the Born approximation term into one representing